Thermal runaway modelling of high-nickel NCA-SCN lithium-ion battery based on thermo-kinetic analysis

Upasana Priyadarshani Padhi[1], Ayushi Mehrotra[1], Yejun Lee[1], Jack J. Yoh[1]
[1]Department of Aerospace Engineering, Seoul National University
Seoul, 08826, South Korea

1 Introduction

The development of next generation lithium-ion battery (LIB) is typically based on nickel rich such as $Li[Ni_xCO_yMn_z]O_2$ (NCM) and $Li[Ni_{(1-x-y)}Co_xAl_y]O_2$ (NCA) cathode material and silicon based anode material such as silicon graphite (SiC), and Silicon carbon nano-composite (SCN). However, higher energy density increases the hazard of a thermal runaway (TR) event as batteries become more energetic [1]. TR can be triggered due to different kinds of abuse viz. electrical, mechanical and thermal abuse. Any hidden defects in the battery may also develop into a TR trigger during the life cycle of the battery [2]. Due to the poor thermal stability of high-nickel LIBs, high temperature can trigger side reactions like the decomposition of the solid electrolyte interphase (SEI) in the temperature range of 70 ℃ to 180 ℃, and reactions between cell components (cathode, anode, electrolyte, and etc.) which are highly exothermic in nature [3]. The heat produced from these exothermic reactions can lead to further increase in the temperature of the battery, causing the TR of the single cell. If the TR phenomenon triggers in multiple cells, it can cause massive damage to the entire system. Therefore, to improve the thermal safety of the LIB system it is critical to have a thorough understanding of the thermal reaction sequence and kinetics of individual and combined materials in order to be able to effectively design and manage high energy batteries. Despite significant efforts to ascertain the thermal behavior of conventional cell components, only few studies have concentrated on high energy materials. Ren *et al.* [4] investigated the exothermic reactions of the six-different battery components of a fully charged (100% state of charge (SOC)) 24 Ah $Li[Ni_{1/3}Co_{1/3}Mn_{1/3}]O_2$/Graphite (NCM/Graphite) battery using differential scanning calorimetry (DSC) technique. Extended-volume accelerated rate calorimetry (EV-ARC) was performed to determine the self-heating process of this battery. A predictive TR model is established based on the kinetic parameters from DSC test showing a good match with adiabatic TR test results. Following to the previous study Wang *et al.* [3] performed thermal analysis on a commercial large-format of high-nickel/silicon–graphite (NCM811/SiC) LIB to build a TR mathematical model based on the detailed side reaction sequence and the reaction kinetics of the battery components to achieve accurate prediction of the TR behavior of the battery. Further, EV-ARC (extended-volume accelerated rate calorimetry) was also carried out to search detectable heat release originated from the side reactions in the cells. The reaction profile thus obtained was used to build a predictive cell TR model. They then further fitted the simulated cell temperature and rate curves with the experimental ones. These studies are remarkable in the battery safety research as these are among the few recent studies which analyze the exothermic reactions between the battery components using the DSC and EV-ARC techniques.

Correspondence to: jjyoh@snu.ac.kr

The present study aims to accurately model the TR phenomena of high nickel lithium-ion battery (NCA88 and SCN) considering the detailed side reactions and corresponding thermal kinetics. The DSC tests are performed by using individual and combined battery components (Anode, Cathode, Anode+Electrolyte, Cathode+Electrolyte, and Cathode+Separator+Electrolyte+Anode) at various heating rate conditions (5 ℃/min, 10 ℃/min, 15 ℃/min, and 20 ℃/min). The thermal kinetics of side reactions are derived from Arrhenius equations by ftting DSC test results and were used to build a predictive TR model.

2 Methodology

2.1 Experiments

In this study, fully charged (SoC 100%: 4.16 V) high-nickel lithium-ion battery samples are used for testing. The high-nickel LIB consists of NCA 88 Li $[Ni_{1-x-y}Co_xAl_y]O_2$ (88% nickel) cathode, a silicon-carbon nanocomposite (SCN) anode, 1.15M Lithium Hexaflurophosphate ($LiPF_6$) with Ethylene Carbonate (EC), Ethyl Methyl Carbonate (EMC), Dimethyl Carbonate (DMC), Vinylene Carbonate (VC), and Vinyl Ethylene Carbonate (VEC) as electrolyte and PA517 as additives. The thermal analyses are performed using DSC 3+ from Mettler Toledo on the individual main components (i.e. the cathode materials, the anode materials, and the electrolyte) and the combined material (anode+electrolyte, cathode+electrolyte and anode+cathode+electrolyte). The sample were put into the HP Steel (reusable) 30 µL pan to hermetically seal and to avoid any interactions with the external environment, 40 ml/min of N_2 gas was flown during the measurement. The tests were performed for a temperature range of 30-640 ℃ under four heat flow rates i.e. 5, 10, 15 and 20 ℃/min (non-isothermal condition).

2.2 Modeling

As a result of the increased temperature, abusive thermal interactions between the positive electrode (NCA 88), negative electrode (SCN), and electrolyte will take place under different temperature ranges and produce a lot of heat and gas, which could result in thermal runaway (TR). A lumped thermal model is used to predict the battery TR behaviors under thermal abuse conditions. The energy balance equation can be written as

$$mC_p \frac{dT(t)}{dt} = Q_{total}(t) \quad (1)$$

Where, $Q_{total}(t) = Q_{reaction}(t) + Q_{dissipation}(t)$ and

$$T(t) = T(0) + \int \frac{dT(t)}{dt} dt \quad (2)$$

Where, M is the total mass, Cp is the heat capacity of cell, $T(t)$ is the cell temperature at time t, $T(0)$ is the initial temperature, Q_{total} is the total heating power. The heat generation during TR is originated from thermo-chemical reactions inside the cell. For any reactant α following reaction step j the heat generation can be determined as

$$Q_{reaction}(t) = \sum_{\alpha,j} Q_{\alpha,j} \quad (3)$$

$$Q_{\alpha,j} = m_{\alpha,j}\Delta H_{\alpha,j} \frac{d\alpha_j(t)}{dt}, \quad (4)$$

Where, $Q_{\alpha,j}$ is the heat generation of one of specific reaction within the cell for instance (cathode, anode, cathode+Ele, anode+ele, and cathode+Anode+ele), $m_{\alpha,j}$ is the mass of reactant, $\Delta H_{\alpha,j}$ is reaction enthalpy of j^{th} reaction. Kinetics analysis of the exothermic reactions in sample Anode+Ele, Cathode+Ele, and Cathode+Anode+Ele is performed based on the DSC tests results under different heating rates (β). DSC heat flow usually displays several exothermic/endothermic peaks representing multiple thermal reaction steps of the materials. In the present study, chemical reaction kinetics on the reaction progress

is provided by applying Friedman isoconverional method to the experimentally obtained DSC data [5] as

$$\beta \frac{d\alpha}{dt} = A_\alpha \exp\left(-\frac{E_\alpha}{RT}\right) f(\alpha) \quad (5)$$

Here, A_α is the frequency factor, $E_{\alpha,j}$ is activation energy, and $f\ (\alpha)$ is the reaction model. The thermal behavior of one reaction step can be determined by the three parameters, such as frequency factor (A_α), activation energy (E_α), reaction enthalpy (ΔH_α) and mechanism function ($f(\alpha)$) of reaction model. Here, to simplify the model the mechanism function is eliminated from eqn. (5) considering zero order reaction model.

3 Results

3.1 Thermal behavior of NCA-SCN LIBs

The thermal behavior of individual and combined materials of the battery are analyzed through DSC thermograms. Figure 1 shows the DSC profile of anode + electrolyte, cathode + electrolyte at different heating rates. The heat flow is normalized by the mass of respective sample materials. From Fig 1(a) a small exothermic can be observed which indicates the decomposition on solid electrolyte interface (SEI) layer at around 70-110 ºC with a heat of reaction equivalent to 407.02 J/g at 15 ºC/min. Anodic SEI has higher reactivity and involves in physical and chemical reactions exothermally in the electrolyte earlier than other material of the cell at about 60-140 °C, followed by the lithiated SNC for the range of heating rate. This is the starting point of exothermic side reactions where SEI layer melts and electrolyte reduction/oxidations degrades the battery material. The following temperature increase lead to reaction between cathode and electrolyte as shown in Fig. 1 (b).

The temperature peak for Cathode+Ele at lower heating rates (5, 10 ºC/min) are insignificant indicating the battery materials are mainly consumed by the electrolyte at lower temperatures and the associated exothermic reactions in the cathode material could not develop thermal runaway for NCA88. However, at higher heating rates the delithiated NCA 88 reacts with electrolyte showing exothermic peaks (with a heat of reaction equivalent to 381.3 J/g at 20 ºC/min) due to the release of gaseous oxygen. Further oxidation with reactive electrolyte components causes subsequent exothermic peaks during the decomposition.

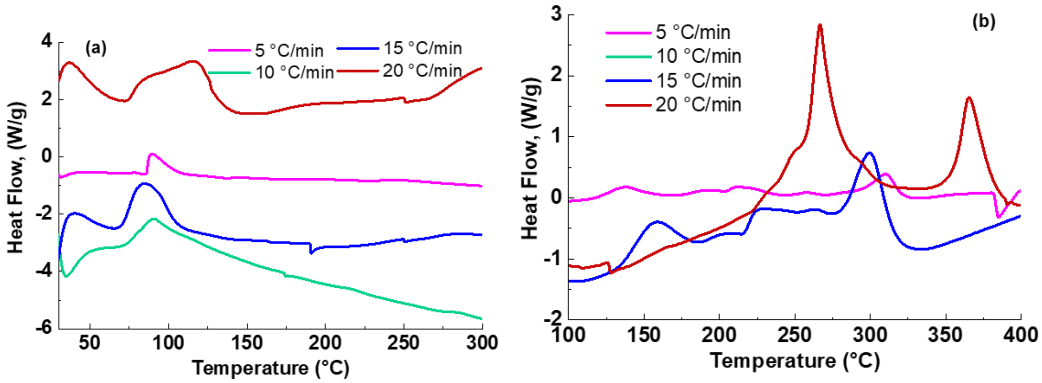

Figure 1: DSC profile of (a) Anode+ele and (b) Cathode+ele at different heating rates.

However, when a mixed sample (anode+cathode+electrolyte) was tested a chain of chemical reaction indicating thermal runaway phenomena is observed. Figure 2 (a)-(d) shows the DSC profile of anode+cathode+electrolyte at various heating rates. Based on the exothermic peaks three different stages of reaction progress is shown in figures (stage 1, stage 2 and stage 3).

Stage 1: decomposition of SEI layer

Stage 2: Self-sustaining reactions which triggers thermal runaway

Stage 3: decomposition of battery materials

Stage 1 shows the decomposition of the SEI layer and reaction between the lithiated anode materials with alkyl carbonates in the electrolyte in a temperature range of around 60-130 °C. Stage 2 shows with further increase in temperature the cathode material undergoes complex phase transformation releasing oxygen as delithiated NCA 88 exhibits strong oxidizability [6]. The amount of oxygen released by the NCA88 is sufficient to oxidize the small fraction of electrolyte releasing tremendous heat. When the amount of heat release is sufficient to sustain further reaction then thermal runaway triggers leading to exponential increase in energy in the form of heat (temperature). In Fig. 2 it can be clearly observed that a TR is observed at 10, 15 and 20 ºC/min. For instance, at 15 ºC/min, the maximum heat generation is 506.5 J/g at 220 °C, indicating thermal runaway. Stage 3 indicates the self-sustained reactions leading to further degradation of battery materials and release of gaseous product. In Fig. 2(a) the endothermic peak is observed because of insufficient heat to self-accelerate the reaction.

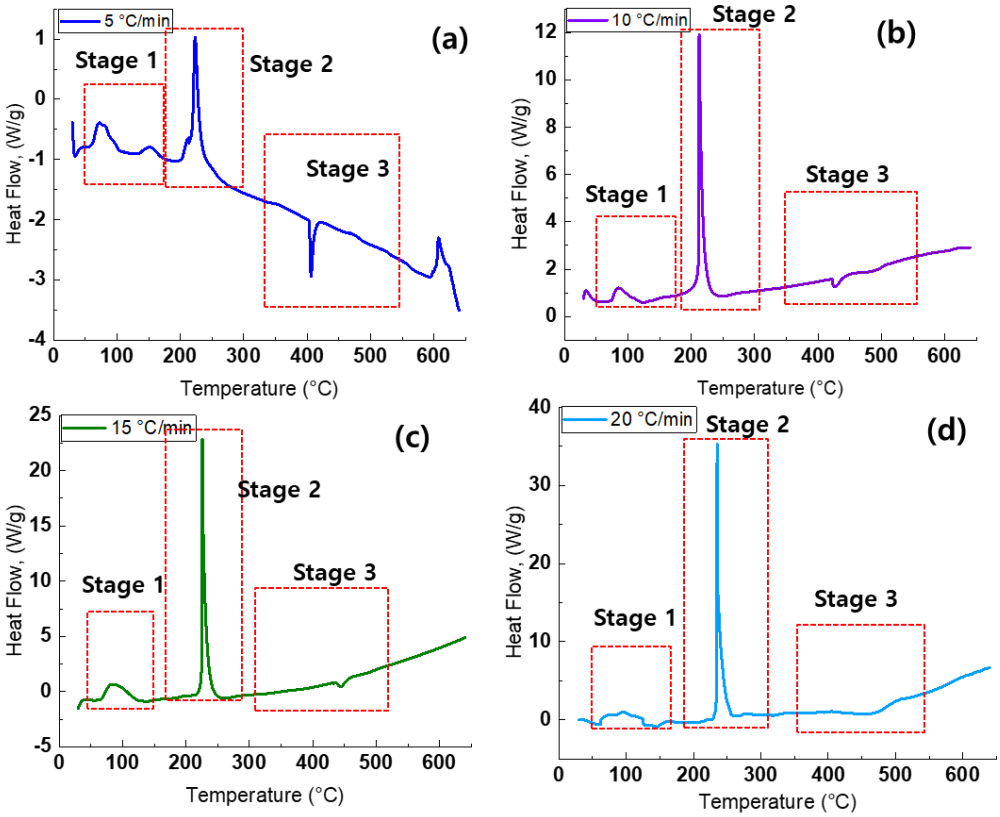

Figure 2: DSC profile of Anode+Cathode+Ele at different heating rates.

Table 1 shows the temperature range of all the stages explained above and corresponding heat generation normalized by the respective sample mass at different heating rate. Thermal runaway is a self-sustained chain reaction phenomena which is accelerated by increase in temperature, in turn releasing energy in the form of heat that further increases temperature. TR occurs at point where an increase in temperature changes the condition in chemical reaction in a way that further increases temperature due to release of tremendous heat due to oxidation reaction. It can be attributed as an uncontrolled positive thermal feedback.

Table 1: Enthalpy of reaction, temperature range, and peak temperature of Cathode+Anode+Ele reaction during thermal runaway.

Heating rate	Stage 1		Stage 2		Stage 3	
(ºC/min)	Q_{reac} (J/g)	T_{range}/T_p (ºC)	Q_{reac} (J/g)	T_{range}/T_p (ºC)	Q_{reac} (J/g)	T_{range}/T_p (ºC)
5	-1220.77	~59-181/	-1101.1	~182-273	-1346.3	~292-577
10	-927.81	~60-165/	-416.8	~ 168-260	269.6	~ 268-576
15	-1067.37	~60-170/	-462.8	~182-260	400.1	~ 270-580
20	-300.227	~60-182/	-597.8	~ 197-292	507.9	~296-584

3.2 Estimation of reaction kinetics based on DSC results

The kinetic parameters (E_α, A_α) of each reaction of battery materials using Kissinger method [7], as follows

$$\ln\left(\frac{\beta_k}{T_{p,k}^2}\right) = \ln\left(\frac{A_\alpha R_0}{E_\alpha}\right) - \frac{E_{a,\alpha}}{R_0 T_{p,k}},\ (k = 1, 2, 3, \ldots..) \quad (6)$$

Where, β_k is the heating rate, $T_{p,k}$ is peak temperature, R_0 is the universal gas constant and k is the number of different heating rates (here 5-20 °C/min). The activation energy E_α, can be determined from the slope of $\ln\left(\frac{\beta_j}{T_{p,j}^2}\right) - \frac{1}{T_p}$ fitting the straight line and the pre-exponential factor A_α can be found from the intercept of the plot. Figure 3 shows the variation of $\ln\left(\frac{\beta_j}{T_{p,j}^2}\right)$ with respect to $\frac{1}{T_p}$ where, the symbols are data from DSC test and lines are best fit for the data using Eqn. (6). Then the heat of reaction can be determined sing Eqn. (4). The obtained kinetic parameters are listed in Table 2.

Table 2: Kinetic and thermal parameters of exothermic reactions

Kinetic parameters	Anode	Cathode	Anode+Ele	Cathode+Ele	Anode+Cathode+Ele
A_α (s^{-1})	4.80E+13	2.80E+16	2.10E+15	2.00E+05	3.48E+06
E_α (J/mol^{-1})	6.10E+04	7.77E+04	8.53E+04	2.83E+04	2.94E+04
ΔH (J/g)	136.3	108.42	-192.056	1622.36	5050.85

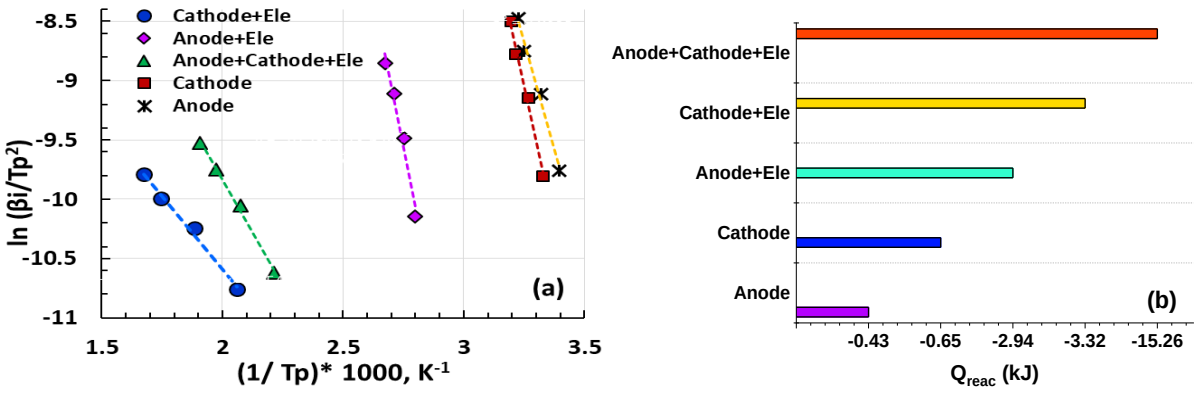

Figure 3: Kinetic parameter calculation using Kissinger's method (a) determination of E_α, $A_{\alpha,}$ (b) heat of reaction at β = 20 ºC/min.

Figure 3 (a) shows the determination of activation energy and pre-exponential factor for individual and combined components at different heating rate obtained using Kissinger's method. Figure 3 (b) presents the calculation result of heat of reaction using Eqn. (4) for the cell components at 20 ºC/min. The cathode+ele releases a total of -3.32 kJ whereas Anode+Cathode+Ele sample demonstrated higher heat release indicating sever reaction between delithiated cathode and electrolyte and then uncontrolled reaction between released oxygen from cathode and electrolyte. However, the release of heat by reductive lithiated anode and oxidative delithiated cathode when reacted with electrolyte indicates thermal abuse could trigger the TR phenomena in the cell. The future study aims to predict the temperature profile by solving Eqn. (1)-(5) and present in detail the thermal runaway qualitatively and quantitatively.

4 Conclusion

The present study investigated the thermal runaway (TR) analysis of high-nickel lithium ion battery (NCA88-SCN) at various heating rate using DSC measurements. The main exothermic reactions and side reactions triggering the TR are determined based on the thermal behavior from DSC profiles of individual and combined battery components. Results show the TR is prone at higher heating rate for a full charged cell leading to catastrophic failure due to reaction between oxidizable delithiated cathode and electrolyte. A cell thermal runaway model was developed based on the interaction dynamics and material kinetics, and the model successfully predicts the thermal runaway behavior. The future work aims to model the temperature profile from the kinetic analyses and present the thermal runaway both qualitative and quantitatively.

References

[1] Liu S, Xu D, Ma T, Wei Z, Lin C, Bai G, et al, Thermal safety studies of high energy density lithium-ion batteries under different states of charge. Int J Energy Res 2020;44(3); 1535-45.

[2] Feng X, Ren D, He X, Ouyang M, Mitigating Thermal Runaway of Lithium-Ion Batteries, Joule 4, 743–770.

[3] Wang Y, Ren D, Feng X, Wang L, Ouyang M, Thermal runaway modelling of large format high-nickel/silicon-graphite lithium-ion batteries based on reaction sequence and kinetics. J. Applied Energy 306 (2022) 117943.

[4] Ren D, Liu X, Feng X, Lu L, Ouyang M, Li J, Model based thermal runaway prediction of lithium-ion batteries from kinetic analysis of cell components J Applied Energy 228 (2018) 633-644.

[5] S. Vyazovkin, K. Chrissafis, M.L.D. Lorenzo, N. Koga, M. Pijolat, B. Roduit, N. Sbirrazzuoli, J.J. Sunol, ICTAC Kinetics Committee recommendations for collecting experimental thermal analysis data for kinetic computations, Thermochimica Acta, 590 (2014) 1-23

[6] Barkholtz HM, Preger Y, Ivanov S, Langendorf J, Torres-Castro L, Lamb J, Ferreira SR. (2019) Multi-scale thermal stability study of commercial lithium-ion batteries as a function of cathode chemistry and state-of-charge. J. Power Sources. 435: 226777.

[7] Kissinger HE. Variation of peak temperature with heating rate in differential thermal analysis. J Res Natl Bur Stand 1934;1956(57):217–21.